# MICRO-SCALE STABILITY OF BUBBLY FLOWS IN PACKED BEDS

Y. SHTEMLER[1], I. SHREIBER[2], M. HERSKOWITZ[2], E. GELMAN[1]

[1]Institute for Industrial Mathematics, 4/24 Yehuda Hanachtom Str.,
Beer-Sheva 84249, Israel , E-mail:shtemler@math.bgu.ac.il
[2] Department of Chemical Engineering, Ben-Gurion University of the Negev,
Beer-Sheva, 84500, Israel

## Abstract

Bubbly liquid downflow through fixed beds and its transition to dispersed-bubble flow is modeled. At the macro (bed) scale the system is described as a compressible fluid filtrating through porous media. The system peculiarities - the isothermal variation of perfect gas in the spherical bubbles, weak compressibility of the liquid etc. - are accounted for at the micro (pore) scale in the state equation. Dimensionless criteria were found determining the bubbly-liquid flow in packings and its micro-scale stability. Part of the criteria were omitted due to their small input, while the rest are contained in a relation following from the micro-level stability criterion: the bubble size growing under a pressure drop across the bed does not exceed the capillary throat. The modeling results are in fair agreement with the experimental data.

## 1. Introduction

Wide-spread approximations for fluid filtration through granular layers consider them as a system of capillaries of an equivalent hydraulic diameter. This allows the main regimes of two-phase flows in fixed beds (Midoux et al 1976, Herskowitz and Smith 1983, Ng 1986, Melli et al 1990, Rode et al 1994, 1995, Mewes et al 1999, Attou et al 1999) to be distinguished at the capillary scale: bubble sizes are (i) sufficiently less than (bubble regime) or (ii) of the order of (dispersed bubble regime) the equivalent hydraulic diameter; continuously distributed gas and liquid phases flow within capillaries (iii) jointly (trickle) or alternately (pulse).

The theoretical studies predicting the flow parameters and criteria for flow-regime changes were mainly concerned with trickle flows. This is due to trickle flow, together with pulse flow, being the main operational regime in fixed beds. However, conditions for the existence of these regimes may also be estimated by stability study of other regimes, e.g. bubbly flow. It is also known that at industrial-scale plants a homogeneous distribution of the phases is difficult to obtain. The local gas and liquid velocities may vary considerably, leading to co-existence of several flow regimes including the bubble flow. Bubble flow described in a relatively simple way can be considered as the reference flow that restricts the location of other regimes on a flow-regime map. Bubble regime presents an interest for elucidation of characteristic parameters and dimensionless criteria in the scale-up problem: extrapolation of measurements made in laboratory-scale reactors to industrial-scale plants. Another reason for such consideration is the fact that acoustic spectra for bubble flows are well studied and can be employed in acoustic monitoring of packed-bed reactors. However, the precise boundary for bubble-to-dispersed-bubble transition is hard to predict experimentally. These regimes can be distinguished rather in a transition zone (Midoux et al 1976, Melli et al 1990, Rode et al 1994, 1995).

The present work is concerned with downward flows of bubbly liquids through fixed beds formed by catalyst particles and with prediction of bubble-to-dispersed-bubble transition. Bubbly liquid filtration in porous media is a quite realistic limit: porous media in various reactors are formed by a capillary system with characteristic size ($10^{-3}$-$10^{-2}$ *m*, Melli et al 1990, Rode et al 1994, 1995) much larger than granular size met in water-filled sands, marine sediments, rocks and petroleum recovery ($10^{-7}$-$10^{-4}$*m*, Anderson and Hampton 1980, Melli et al 1990). This justifies our subsequent analysis of the capillary size being sufficiently larger than the characteristic size of micro-bubbles. The basic approaches to predicting flow-regime changes in such systems are stability studies at macro-level (bed-scale) and micro-level (pore-scale). The idea of micro-level instability in fixed beds was employed previously as a semi-empirical approach to predicting trickle-to-pulse transitions caused by perturbed liquid films blocking the capillaries (Sicardi et al 1979, Sicardi and Hofmann 1980, Ng 1986). Prediction of flow-regime changes in packed beds, design, scale-up and operation of industrial reactors with the help of experimentally obtained flow regime maps is often complicated due to their dimensional form and incomplete data on experimental conditions. This is related to the large number of the determining physical, operating and design parameters and to the lack of knowledge on the basic dimensionless criteria. In the present study corresponding dimensionless criteria were derived describing the bubbly liquid flow in porous media and its micro-level stability. We develop an approach avoiding hydraulic and dimensional grounds to predicting bubble-to-dispersed-bubble transition caused by the bubbles blocking the capillaries due to their growth under a pressure drop across the bed. It provides for the region of possible existence of bubbly regimes inside which classical macro-level analysis should be carried out. The proposed model does not consider the main flow instability under the growth of perturbations, but studies variation of the main flow up to overstepping the boundaries of its applicability. Micro-level study does not replace classical analysis of macro-level instabilities of the main flow, but makes it unnecessary where the main flow loses meaning.

## 2. Modeling of bubble flows in packings

The chemical reactions and the effects of phase transitions, the bed elasticity, buoyancy and surface tension are not taken into account. At the macroscopic level bubbly flows are considered in the Brinkman approximation as a compressible fluid filtrating through porous media

$$\rho \frac{D\vec{U}}{Dt} = -\frac{\mu}{k}\vec{U} - \vec{\nabla}P + \mu \nabla^2 \vec{U}, \qquad \frac{D\rho}{Dt} + \rho \vec{\nabla}\vec{U} = 0, \quad \frac{D}{Dt} = \frac{\partial}{\partial t} + \vec{U}\vec{\nabla}. \qquad (1)$$

Note that at normal conditions in air-water systems the surface tension becomes significant for small bubbles with radii of the order of or less than $10^{-6}$ *m*, and here we neglect this effect assuming the bubbles to be sufficiently large. In the bubble regime the liquid and gas bubbles move with a common velocity (Ng 1986) and we assume the bubbles to be frozen into the liquid. Here $\vec{U}$, $P$ and $\rho$ are interstitial velocity, pressure and density of the mixture within a pore, $\vec{\nabla}$ is the differential operator, $D/Dt$ is the substantial derivative, $t$ is time; $k = d_p^2/180 \cdot m^2/(1-m)^2$ is the permeability coefficient, $m = const$ is porosity, $d_p$ is the diameter of solid spherical particles forming the bed. The effective dynamic viscosity of the mixture $\mu$ is approximated by a dependence on the gas volume

fraction $j_g$, which can be determined experimentally or theoretically. Thus, for sufficiently small gas-volume fractions Batchelor (1967) derives for the ratio of the mixture-to-liquid viscosity

$$\frac{m(j_g)}{m_l} = 1 + j_g . \tag{2}$$

The number of solid particles on the reactor diameter is assumed to be sufficiently large for the wall friction to be negligible. The viscous effects are neglected everywhere below at the macroscopic level, except the resistance force

$$r\frac{D\vec{U}}{Dt} = -\frac{m}{k}\vec{U} - \vec{\nabla}P . \tag{3}$$

If the inertial term in the left-hand part of Eq. (3) is neglected, the Darcy approximation takes place:

$$\vec{U} = -\frac{k}{m}\vec{\nabla}P . \tag{4}$$

The effect of bulk viscosity as well as micro-level inertia effects of a bubbly liquid should be taken into account below by a cell model. A state equation is derived accounting for the system peculiarities at the microscopic level: the weak compressibility of the liquid and the isothermal variation of perfect gas in the bubbles

$$P - P_g^{(r)} = \tag{5}$$

$$r_l R^{(r)2}\left[-\frac{D^2 q}{Dt^2}F_1(q,Q^{(r)}) + \left(\frac{Dq}{Dt}\right)^2 F_2(q,Q^{(r)})\right] - m_l\frac{Dq}{Dt}F_3(q,Q^{(r)}) - P_g^{(r)}F_4(q,Q^{(r)},a) .$$

Here $P_g$ is the gas pressure in the spherical bubbles with radius $R$, subscripts $g$ and $l$ denote parameters of the gas and liquid, the superscript $r$ marks the quantities at an arbitrary reference state at which a homogeneous bubbly liquid exists. Equation (5) is the Rayleigh equation for dynamics of the isolated bubble generalized for the bubbly liquid mixture. Coefficients $F_j$ ($j$=1, 2, 3, 4) are expressed through the gas/liquid volume fraction $Q = j_g / j_l$ at the reference state $Q^{(r)}$, its current normalized value $q$ and parameter $a$ characterizing the compressibility of the liquid:

$$F_1(q,Q^{(r)}) = \frac{1 - j_g^{1/3}(q,Q^{(r)})}{3q^{1/3}},\ F_2(q,Q^{(r)}) = \frac{1 - j_g^{4/3}(q,Q^{(r)})}{18q^{4/3}},\ F_3(q) = \frac{4}{3q},$$

$$F_4(q,Q^{(r)},a) = (1+Q^{(r)})\sqrt{a^2-1}\arctan\frac{(q-1)\sqrt{a^2-1}}{[(1+Q^{(r)})a^2-1]q+1}, \tag{6}$$

$$j_g(q,Q^{(r)}) = \frac{qQ^{(r)}}{1+qQ^{(r)}},\ q = \frac{Q}{Q^{(r)}},\ a = \sqrt{1 + \frac{a_l^2 r^{(r)}}{P_g^{(r)}}\frac{Q^{(r)}}{1+Q^{(r)}}}. \tag{7}$$

Here $a \equiv a_l / a^{(r)}$, $a_l \equiv const$ is liquid sound velocity, $a$ is the mixture sound velocity accounting for the weak compressibility of the liquid. Equations (6) have been derived with the help of the following relations for the gas pressure, bubble radius and mixture density:

$$\frac{P_g}{P_g^{(r)}} = 1 - F_4(q,Q^{(r)},a),\ \frac{R}{R^{(r)}} = q^{1/3},\ \frac{r}{r^{(r)}} = \frac{1+Q^{(r)}}{1+qQ^{(r)}} . \tag{8}$$

The unreal feature of the state equation (5) with an incompressible liquid phase, which is that in the

steady-state mixture $P_g$ tends to infinity as $j_g$ vanishes, is modified by accounting for the weak compressibility of the liquid. Weak compressibility of the liquid is assumed to be negligible, i.e. $r_l = r_{l,0} \equiv const$, everywhere except the problem for bubble pressure:

$$\frac{dP_g}{dr(q)} = a^2(r(q)),\ P_g = P_g^{(r)} \text{ at } q = 1. \tag{9}$$

$$\frac{1}{a^2} = \frac{1}{a_l^2} + \frac{1}{a_0^2},\ a_0^2 = \frac{dP_{g,0}}{dr(q)} \equiv \frac{P_g^{(r)}}{r^{(r)}} \frac{(1+qQ^{(r)})^2}{(1+Q^{(r)})Q^{(r)}q^2},\quad \frac{qP_{g,0}}{(1+Q^{(r)}q)r} = \frac{P_g^{(r)}}{(1+Q^{(r)})r^{(r)}}.$$

The subscript 0 denotes the quantities calculated in neglect of the liquid compressibility.

A one-dimensional flow along the *x*-direction satisfies the following initial and boundary conditions:

$$q = q^{(in)}(x),\ \vec{U} = \vec{U}^{(in)}(x) \text{ at } t = 0,\ P = P^{(i)}(t),\ q = q^{(i)}(t) \text{ at } x = 0,\ P = P^{(o)}(t) \text{ at } x = H. \tag{10}$$

Here $H$ is the bed length, the superscripts *i/o* and *in* mark the inlet/outlet and initial quantities, the bed inlet/outlet values are assumed to be constant.

We also assume that a homogeneous mixture of a bubbly liquid actually exists at the bed inlet and define the mixture parameters at the bed inlet as reference:

$$Q^{(r)} = Q^{(i)},\ R^{(r)} = R^{(i)}, P_g^{(r)} = P^{(i)}, r^{(r)} = r^{(i)}. \tag{11}$$

The inlet gas/liquid volume fraction, bubble radius, mixture density and pressure are assumed to be known. The inlet mixture density can be expressed through the inlet gas density, gas/liquid volume fraction and liquid density:

$$\frac{r^{(i)}}{r_{l,0}} = \frac{1}{1+Q^{(i)}}(1 + Q^{(i)}\frac{r_g^{(i)}}{r_{l,0}}).$$

### 3. Dimensionless formulation of the problem

The problem was made dimensionless with the help of the following characteristic scales for length, pressure and density as well as for the characteristic time and velocity:

$$H^* = H,\ P^* = P^{(i)} - P^{(o)},\ r^* = r_{l,0},\ t^* = H^*\sqrt{r^*/P^*},\ U^* = H^*/t^*. \tag{12}$$

Dimensionless quantities are defined as follows:

$$\vec{U}' = \vec{U}t^*/H^*, P' = (P - P^{(o)})/P^*,\ r' = r/r^*,\quad t' = t/t^*,\ x' = x/H^*, \vec{\nabla}' = H^*\vec{\nabla}\ ,\ m' = m/m_l \tag{13}$$

Omitting the superscript prime everywhere below, using expressions (11) for reference values and employing the same notations for dimensionless as for dimensional quantities, we rewrite relations (1), (5) and (10):

$$p_1\frac{D\vec{U}}{Dt} = -(1+p_0q)[m(p_0q)\vec{U} + p_1\vec{\nabla}P],\ p_0\frac{Dq}{Dt} - (1+p_0q)\vec{\nabla}\vec{U} = 0, \tag{14}$$

$$P - 1 = [-F_1(q,p_0)\frac{D^2q}{Dt^2} + F_2(q,p_0)(\frac{Dq}{Dt})^2]p_2^2 - p_3F_3(q)\frac{Dq}{Dt} - \frac{1}{p_4}F_4(q,p_0,a(p_0,p_5)), \tag{15}$$

$$q = q^{(in)}(x),\ \vec{U} = \vec{U}^{(in)}(x) \quad \text{at } t = 0,\quad q = 1,\qquad P = 1 \quad \text{at } x = 0,\qquad P = 0 \quad \text{at } x = 1. \tag{16}$$

Here $p_j$ ($j$=0, 1, 2, 3, 4, 5) are dimensionless criteria, $F_j$ ($j$=1, 2, 3, 4) are given by Eqs. (6), but now depend on the normalized gas/liquid volume fraction $q$ and dimensionless criteria $p_j$ ($j$ = 0, 1, , 5), which in their turn are expressed through modified dimensionless criteria $\Pi_j$ ($j$ = 0, 1, , 6):

$$a = \sqrt{1 + \frac{p_0}{(1+p_0)^2}\frac{1}{p_5^2}},\ \frac{p_0}{\Pi_0} = 1, \frac{p_1}{\Pi_1} = \sqrt{\frac{\Pi_4}{1-\Pi_4}} \cdot (1 + \Pi_0\Pi_6),$$

$$\frac{p_2}{\Pi_2} = 1,\ \frac{p_3}{\Pi_3} = \sqrt{\frac{1-\Pi_4}{\Pi_4}}, \frac{p_4}{\Pi_4} = 1,\ \frac{p_5}{\Pi_5} = \frac{1}{\sqrt{1-\Pi_4}} \cdot \frac{1}{\sqrt{1+\Pi_0\Pi_6}}.$$

The criterion $\Pi_0$ equals the inlet gas/liquid volume fraction, $\Pi_1$ and $\Pi_2$ characterize inertia effects at the macro- and micro- levels, $\Pi_3$ describes viscous dissipation at the micro-level. The criterion $\Pi_4$, one of the main parameters of the system, is the pressure drop across the bed. The criterion $\Pi_5$ characterizes the liquid compressibility, $\Pi_6$ equals the ratio of the inlet gas density to the liquid density

$$\Pi_0 = Q^{(i)}, \Pi_1 = \frac{k}{H}\frac{\sqrt{P^{(o)} r_{l,0}}}{m_l}, \Pi_2 = \frac{R^{(i)}}{H},\ \Pi_3 = \frac{m_l}{H\sqrt{P^{(o)} r_{l,0}}},$$

$$\Pi_4 = \frac{P^{(i)} - P^{(o)}}{P^{(i)}},\ \Pi_5 = \frac{1}{a_l}\sqrt{\frac{P^{(o)}}{r_{l,0}}},\ \Pi_6 = \frac{r_g^{(i)}}{r_{l,0}}. \qquad (17)$$

The modified dimensionless criteria $\Pi_j$ ($j$=0, 1, 2, 3, 4, 5, 6) are introduced above in order to extract explicitly the inlet pressure drop $P^{(i)}$ from the criteria $p_j$ ($j$=1, 2, 3, 4, 5) naturally obtained after the problem is made dimensionless with the pressure drop $P^{(i)}$ - $P^{(o)}$ as the characteristic value. This is done for convenience of comparison with experimental data in which the outlet pressure is usually fixed, while the inlet pressure can vary in a wide range.

To simplify our consideration by reducing the number of determining parameters, the ratio of the gas/liquid density is assumed to be small (so that $\Pi_0\Pi_6 << 1$), and $\Pi_6$ is neglected elsewhere below except the right-hand part of the former of relations (27) proportional to $\Pi_6$. In particular, we set in the above relations

$$1 + \Pi_0\Pi_6 \approx 1,\ a \approx \sqrt{1 + \frac{\Pi_0}{\Pi_5^2}\cdot\frac{1-\Pi_4}{(1+\Pi_0)^2}}.$$

Since $\Pi_5$ is small and only enters the problem through the value of $a$, the latter should be of the order of unit for the input of the liquid compressibility to be significant. This yields that $\Pi_0 / \Pi_5^2$ should be of the order of or less than unit, and a characteristic value of $\Pi_0 \sim \Pi_5^2$. The characteristic dimensionless criteria depending on the inlet bubble radius $R^{(i)}$ (Table 3) and independent on $R^{(i)}$ (Table 2) are calculated for typical physical, geometrical and operating data presented in Table 1. In Table 1 the air-water system is considered, the bed parameters, $d_p = 5\cdot10^{-3}$ $m$ and $H$ =1.3 $m$, correspond to experiment conditions by Rode et al (1994, 1995), for other parameters some typical values are taken in order to estimate the characteristic values of dimensionless criteria presented in Tables 2 and 3. Under real conditions, the inlet pressure, for instance, can be varied in a wide range within the interval $0 < (P^{(i)} - P^{(o)})/P^{(i)} < 1$, as it will be considered below. Dimensionless stability

criterion $\Pi_* = (R^{(i)}/(0.11 \cdot d_p))^3$ in Table 3 will be introduced below (see Eq. (22)). The criteria varied with the inlet bubble radius are selected in the separate Table 3 for convenience of comparison with experimental data in which the inlet radius is usually uncontrolled.

Table 1. Physical, geometrical and operating parameters

| $r_{l,0}$ $kg \cdot m^{-3}$ | $m_l$ $Pa \cdot s$ | $a_l$ $m \cdot s^{-1}$ | $m$ – | $d_p$ $m$ | $H$ $m$ | $P^{(i)}$ $Pa$ | $P^{(o)}$ $Pa$ | $r_g^{(i)}$ $kg \cdot m^{-3}$ |
|---|---|---|---|---|---|---|---|---|
| $10^3$ | $10^{-3}$ | $1.5 \cdot 10^3$ | 0.4 | $5. \cdot 10^{-3}$ | 1.3 | $2 \cdot 10^5$ | $10^5$ | 1.8 |

Table 2. Dimensionless criteria independent of the inlet bubble radius

| $\Pi_0$ | $\Pi_1$ | $\Pi_3$ | $\Pi_4$ | $\Pi_5$ | $\Pi_6$ |
|---|---|---|---|---|---|
| $10^{-4}$ | 0.46 | $0.8 \cdot 10^{-7}$ | 0.5 | $0.94 \cdot 10^{-2}$ | 0.002 |

Table 3. Dimensionless criteria dependent on the inlet bubble radius

| $10^4 \cdot 2R^{(i)}[m]$ | 4.0 | 7.0 | 8.8 | 10.0 | 10.8 | 10.92 | 10.96 |
|---|---|---|---|---|---|---|---|
| $10^4 \Pi_2$ | 1.5 | 2.7 | 3.4 | 3.8 | 4.15 | 4.20 | 4.22 |
| $\Pi_*$ | 0.05 | 0.25 | 0.5 | 0.75 | 0.95 | 0.98 | 0.99 |

**4. Analysis of micro-level stability**

The system under consideration has characteristic scales of length which strongly differ in the order of values: the macro scale equals the bed length, and the micro scales characterize the sizes of the bed pores and bubbles. Thus, criteria $\Pi_j$ ($j$=1,2,3) are inversely proportional to the bed length $H$. However, the criterion $p_1 \sim \Pi_1$ =0.46 is not quite small for the data presented in Table 1, so the wide-spread Darcy approximation established for asymptotically small values of the macro-inertia criterion $p_1 \sim \Pi_1$ in Eqs. (14) – (16) may be used with relatively low accuracy. Note that the value of $\Pi_1$ strongly depends on the granular sizes, thus if we consider the typical value $d_p = 3 \cdot 10^{-3}$ $m$ as in experiments by Midoux et al (1976), instead of $d_p = 5 \cdot 10^{-3}$ $m$ presented in Table 1 for the data by Rode et al (1994,1995), we obtain the value of $\Pi_1$=0.18 instead of $\Pi_1$=0.46. The criteria $p_2 = \Pi_2 \sim 10^{-4}$ and $p_3 \sim \Pi_3 \sim 10^{-7}$ are extremely small in fact. This implies that the terms with substantial derivatives in the state equation, proportional to $p_2 = \Pi_2$ and $p_3 \sim \Pi_3$, can be significant only at sharp and/or rapid variations of the flow which can occur near the bed boundaries, at fronts or at fast oscillations etc. Below we assume the possibility to neglect the corresponding terms and the

present study is concerned with the filtration process after the completion of the bed load, with no filtration fronts, sharp and rapid variations. Then, the terms marked by $\Pi_2$ and $\Pi_3$ may be ignored in the state equation (15), and after substitution of $F_4$ we obtain the relation between the pressure and the normalized gas/liquid volume fraction of the mixture:

$$P(q)-1 = -\frac{(1+\Pi_0)\sqrt{a^2-1}}{\Pi_4}\arctan\frac{(q-1)\sqrt{a^2-1}}{(1+\Pi_0)a^2q+1-q}, \tag{18}$$

$$a(\Pi_0,\Pi_4,\Pi_5)=\sqrt{1+\frac{\Pi_0}{\Pi_5^2}\cdot\frac{1-\Pi_4}{(1+\Pi_0)^2}}\ .$$

According to Eqs. (7), (8), $dr/dq<0$. Hence,

$$\frac{dP}{dq}=a^2\frac{dr}{dq}<0 \text{ or } \frac{dq}{dP}=\frac{1}{a^2}\frac{dq}{dr}<0, \tag{19}$$

i.e. the normalized gas/liquid volume fraction $q$ should increase with the pressure drop. Assume the pressure drop monotonicity across the bed ($dP/dx<0$), which is quite natural from the physical point of view and may be verified by direct numerical simulations of the entire problem. Then the normalized gas/liquid volume fraction $q$ monotonically increases across the bed up to its maximal value $q^{(o)}$ at the bed outlet, where according to the boundary condition (16) pressure has the minimal value $P=0$. In fact the gas fraction cannot rise infinitely since the bubble size increases with it, and the bubble diameter $2R$ cannot exceed the minimal throat diameter of the capillary $d_{thr}$, otherwise a flow regime change occurs, the bubbly regime will be unstable and we have the stability condition:

$$2R \le d_{thr}. \tag{20}$$

Here the throat diameter $d_{thr}$ as well as the equivalent hydraulic diameter $d_e$ of the capillary are expressed through the particle diameter $d_p$ (see e.g. Ng 1986)

$$d_{thr}=b_{thr}\cdot d_p,\quad d_e=\left(\frac{m}{1-m}\right)^{1/3}d_p\ . \tag{21}$$

We assume the ratio of the capillary throat to the equivalent hydraulic diameter $b_{thr}=\sqrt{\sqrt{3}/p-1/2}\approx 0.22$ to be sufficiently small in order to apply the above stability condition within our approach. The gas fraction $q$ remains as finite as the bubble radius $R$, it cannot exceed a critical value (see Eqs. (8), (16) and condition (20))

$$1\le q\le q^{(o)}\le 1/\Pi_*\ . \tag{22}$$

The stability criterion $\Pi_*$ adopted here is not dependent on any empirical factors, but only on sizes of the inlet bubbles and bed particles

$$\Pi_*=\left(\frac{2R^{(i)}}{d_{thr}}\right)^3\equiv\left(\frac{2R^{(i)}}{0.22d_p}\right)^3.$$

Relation (18) resolved explicitly with respect to $q$ yields

$$q=\frac{\sqrt{a^2-1}+T}{\sqrt{a^2-1}-(a^2-1+a^2\Pi_0)T},\ T=\tan\frac{(1-P)\cdot\Pi_4}{(1+\Pi_0)\sqrt{a^2-1}}. \tag{23}$$

Since at first micro-level instability occurs at the bed outlet, substitution of Eq. (23) into (22) yields that $q^{(o)}\le 1/\Pi_*$ at $P=0$ if

$$\frac{(1+\Pi_0)a^2T_* - (T_* + \sqrt{a^2-1})(1-\Pi_*)}{\sqrt{a^2-1} - (a^2-1+a^2\Pi_0)T_*} \le 0, \qquad T_* = \tan\frac{\Pi_4}{(1+\Pi_0)\sqrt{a^2-1}}. \tag{24}$$

Inequality (24) provides for the regions of stable and unstable regimes in the plane $\{\Pi_0 = Q^{(i)}, \Pi_4 = (P^{(i)} - P^{(o)})/P^{(i)}\}$ at given criteria of liquid compressibility $\Pi_5$ and stability $\Pi_*$.

The regions of instability in the plane $\{\Pi_0, \Pi_4\}$ are bounded by two curves, transition (solid) and limiting (dotted), determined by conditions for the change of signs of the numerator and denominator in (24)

$$\Pi_4 = (1+\Pi_0)\sqrt{a^2-1}\arctan\frac{(1-\Pi_*)\sqrt{a^2-1}}{\Pi_* + a^2 - 1 + a^2\Pi_0}, \ \Pi_4^{(a)} = 1-\Pi_* \tag{25}$$

$$\Pi_4 = (1+\Pi_0)\sqrt{a^2-1}\arctan\frac{\sqrt{a^2-1}}{a^2-1+a^2\Pi_0}, \ \Pi_4^{(a)} = 1 \tag{26}$$

with $a(\Pi_0, \Pi_4, \Pi_5) = \sqrt{1 + \frac{\Pi_0}{\Pi_5^2}\cdot\frac{1-\Pi_4}{(1+\Pi_0)^2}}$.

In the limit of incompressible liquid ($\Pi_5 << 1$, so that $a >> 1$) these curves are reduced asymptotically to the horizontal straight lines marked by superscript *a*. The regions of instability can easily be established by noting that the numerator is negative, while the denominator is positive at $\Pi_4 = 0$ (i.e. at $T_* = 0$). Equations (26) for limiting curves may be derived directly from Eqs. (25) for transition curves by setting $\Pi_*$=0. Equations (25), (26) provide for the implicit dependence $\Pi_4 = \Pi_4(\Pi_0, \Pi_5, \Pi_*)$, where the criterion $\Pi_5$ is usually fixed in any system. In Fig. 1 the regions of instability in the plane $\{\Pi_0, \Pi_4\}$ bounded by transition (solid) and limiting (dotted) curves are shown together with the horizontal asymptotes corresponding to the limit of incompressible liquid ($\Pi_5 << 1, a >> 1$). The influence is illustrated of criteria $\Pi_5$ and $\Pi_*$, the numerical values of which mark the solid and dotted curves. In the bubbly regime the gas volume fraction $j_g$ is usually less than 0.5 and the results of simulations are presented in Fig. 1 for $\Pi_0 = Q^{(i)} \equiv j_g^{(i)}/(1-j_g^{(i)}) < 1$. Fig. 1 shows that the liquid compressibility significantly influences the micro-level stability of bubbly flows at gas volume fractions, $j_g^{(i)}$, less than 0.5 ($Q^{(i)} < 1$). For any given system the criterion $\Pi_5$ has a fixed value, for instance, $\Pi_5 = 0.0067$ for the air-water mixture, while the criterion $\Pi_*$ can be varied due to variations of the inlet bubble radius.

Note that the above analysis of micro-level stability requires neither finding the flow velocity and mixture density distributions across the bed, nor knowledge of the bed length. It provides for the transition curves for bubble-to-dispersed-bubble flow in the plane of the pressure drop and gas/liquid volume fraction at known physical properties of the phases, bed-particle sizes and the inlet bubble radius.

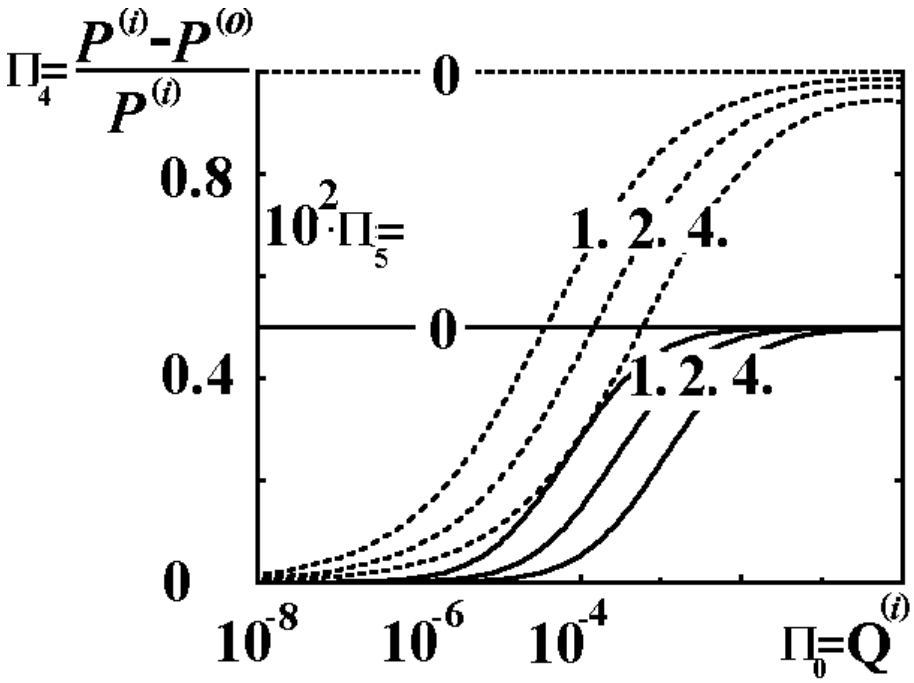


Figure 1. Influence of the liquid compressibility criterion $10^2 \cdot \Pi_5 \equiv \frac{1}{a_l}\sqrt{\frac{P^{(o)}}{r_{l,0}}}$ =0., 1., 2., 4.

Pressure drop vs the ratio of gas/liquid volume fractions, $\Pi_* \equiv (\frac{2R^{(i)}}{d_{thr}})^3$ =0.5.

— transition curves separating stable (below) and unstable (above) bubbly regimes,

---- limiting curves separating unstable (below) and non-existent (above) bubbly regimes,

(solid and dotted horizontal straight lines correspond to the limit of incompressible liquid).

**5. Comparison with experimental data**

The experimental flow-regime maps can significantly differ from author to author, which is commonly explained by the fact that different interpretations are used for the flow-regime transition (Ng 1986). For bubble-to-dispersed-bubble transition reliable experimental data have not been found by Ng (1986) at all. A semi-empirical correlation proposed by him for the transition curve in the plane of the dimensional superficial mass-flow rates of gas and liquid is based on a given constant value of liquid saturation. In fact, liquid saturation depends on both gas and liquid flow rates, and Rode et al recently published some experimental data for bubbly regimes (1994, 1995). However, they could not describe precisely the transition curve for bubble-to-dispersed-bubble regime. This is because the bubble flow with more or less spherical bubbles in a liquid stream can be distinguished from the dispersed-bubble flow, where the bubbles deform and elongate rather in a transition zone than at the transition curves (see also the corresponding experimental data by Midoux et al 1976 and Melli et al 1990).

Two circumstances hamper comparison of the modeling results with empirical correlations. On the

one hand, the available experimental flow-regime maps are given without indicating some frequently uncontrolled parameters necessary for comparison with the results of theoretical modeling. For instance, the bubble flow in experimental flow-regime maps is presented with no mention of the inlet radius of the bubbles - one of the main parameter characterizing the system instability. On the other hand, our model does not use mass and momentum equations providing for the knowledge of the superficial gas and liquid mass-flow rates. The bubbly regime micro-level stability is fully described by the above criterion derived in terms of the pressure drop and the inlet gas/liquid volume fraction. However, under experimental conditions the superficial gas and liquid mass-flow rates are known rather than the inlet pressure (or, equivalently, the pressure drop across the bed). The solution of the entire problem is necessary for comparison with experimental flow-regime maps presented in the plane of the dimensional superficial gas and liquid mass-flow rates by Rode et al (1994, 1995). The relation between these values requires a solution of the complete problem. To avoid this in comparison of experimental correlations with the modeling results, we assume that the Darcy approximation (4) $U = -\frac{k}{m}\frac{\partial P}{\partial x}$ is valid, estimate dimensional superficial mass-flow rates through their values at the bed inlet $G = m j_g^{(i)} r_g^{(i)} U^{(i)}$, $L = m j_l^{(i)} r_{l,0} U^{(i)}$ and restrict ourselves by the simplest estimate for the inlet pressure gradient $(\frac{\partial P}{\partial x})^{(i)} \approx -\frac{P^{(i)} - P^{(o)}}{H}$. Superficial mass-flow rates at the bed inlet rewritten in dimensionless form are as follows:

$$\frac{G}{m\sqrt{P^{(o)} r_{l,0}}} = \frac{\Pi_1 \Pi_6}{m(\Pi_0)} \frac{\Pi_0}{1+\Pi_0} \frac{\Pi_4}{1-\Pi_4}, \quad \frac{L}{m\sqrt{P^{(o)} r_{l,0}}} = \frac{\Pi_1}{m(\Pi_0)} \frac{1}{1+\Pi_0} \frac{\Pi_4}{1-\Pi_4}. \tag{27}$$

The transition and limiting curves in the plane of {*G*, *L*} are determined in the parametric form (with the parameter $\Pi_0$ varying along the curves) by setting in these relations the unknown function $m(\Pi_0)$ equal to unit (this is approximately valid for small $\Pi_0$, see Eq. (2)) and substituting Eqs. (25), (26) for $\Pi_4$.

In Fig. 2 the inlet bubble radius (or, equivalently, the value of the stability criterion) is identified corresponding to the experimentally observed transition from the bubble-to-dispersed-bubble flow.

In Fig. 2 comparison is carried out of the modeling results with experimental data by Rode et al (1994, 1995) for different values of the stability criterion $\Pi_*$=0.95, 0.98, 0.99 ($2R^{(i)}/d_{thr}$=0.983, 0.993, 0.996, respectively). From the experiments by Rode et al (1994, 1995) in which the bubble flow occurs at $G<0.02 kg \cdot m^{-2} s^{-1}$ the diameter of the inlet gas bubbles corresponding to the transition of the bubble-to-dispersed-bubble regime should be chosen in our modeling within $0.993< 2R^{(i)}/d_{thr}<0.996$ ($0.98< \Pi_*<0.99$, $d_{thr} = 1.1 \cdot 10^{-3} m$, $d_p = 5 \cdot 10^{-3} m$). From experimental studies by Rode et al (1994, 1995) it can be concluded that the bubble-to-dispersed-bubble transition occurs when the inlet diameter of the gas bubbles is close to the throat diameter of the capillaries and the gas-volume fraction is close to 0.5.

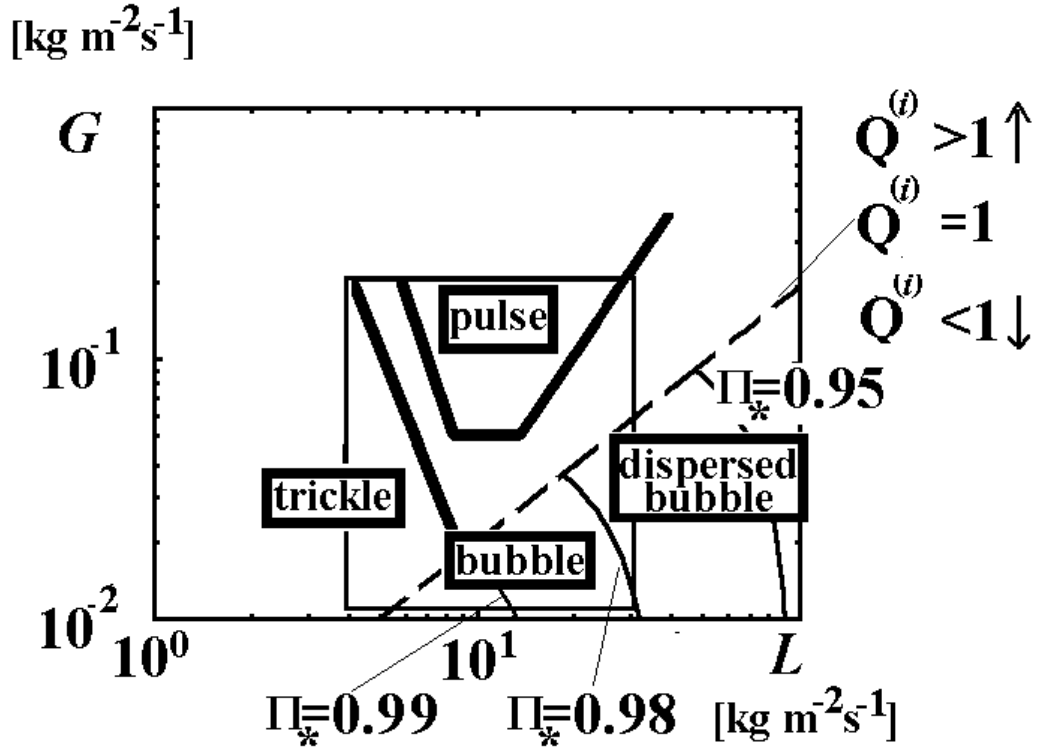


Figure 2. Comparison of the present modeling at $\Pi_* \equiv (\frac{2R^{(i)}}{d_{thr}})^3$ =0.95, 0.98, 0.99 with the experimental results adapted from Rode et al (1994, 1995) , $d_p = 5 \cdot 10^{-3}\ m$, $H$ = 1.3 $m$. Dimensional superficial mass-flow rate of gas vs that of liquid.

$$\Pi_1 \equiv \frac{k}{H}\frac{\sqrt{P^{(o)} r_{l,0}}}{m_l} = 0.46,\ \Pi_5 \equiv \frac{1}{a_l}\sqrt{\frac{P^{(o)}}{r_{l,0}}} = 0.0067,\ \Pi_6 \equiv \frac{r_g^{(i)}}{r_{l,0}} = 0.002.$$

transition curves separating experimentally observed flow regimes,
location of domains of the experimentally observed regimes of flow,
— transition curves separating stable-bubble flow (left) and unstable-dispersed-bubble flow (right),
- - - straight line $Q^{(i)} = 1$, above which $Q^{(i)} > 1$, i.e. $j_g^{(i)} > 0.5$, below - $Q^{(i)} < 1$, $j_g^{(i)} < 0.5$.
domain investigated experimentally by Rode et al (1994, 1995).

**6. Summary**

The bubbly flows through porous media can be unstable at the micro-level, the transition occurs from bubble-to-dispersed-bubble regime. The transition curves are obtained depending on the system parameters. The liquid compressibility can significantly influence the micro-level stability of bubbly flows at sufficiently small gas volume fractions. There is a strong dependence of the transition curve on the inlet bubble radius (or, equivalently, the value of the stability criterion). The bubble radius at the bed inlet is found to be one of the main parameters in the bubble regime of flow and the single parameter uncontrolled in the available experimental data. Under real conditions the inlet value of the bubble radius depends on the way the bubble-liquid mixture is prepared. If the bubbly liquid is

prepared by a super-saturation technique, the inlet bubble size can be varied in a wide range, while if it is produced by mixing the gas and liquid in a chamber beyond the bed inlet, the inlet bubble size is hard to predict. Comparison of the present modeling for the bubble-to-dispersed-bubble transition with the available experimental data for the latter type of system provides for their proximity when the inlet bubble diameter is close to the diameter of the throat of the packing capillaries. According to the present analysis pressure elevation leads to a rise in micro-level instability. Characteristic parameters and dimensionless criteria derived in the present work may be useful in the scale-up problem. The modeling results for the micro-level mechanism of bubble-to-dispersed-bubble transition are in fair agreement with the experimental data by Rode et al (1994, 1995) for the inlet-bubble diameter a little less than the throat diameter of the capillary channel and for the inlet gas-volume fraction close to 0.5.

*Acknowledgment*

Support of the Israel Ministry of Science (Grant N8565-98) is gratefully acknowledged.

**References**

Anderson A. .L., & Hampton L.D. (1980). Acoustics of gas-bearings sediments. I, II. *J. Acoust. Soc. Am.*, 67(6), 1865 – 1889.

Attou A., Boyer C., & Ferschneider G., (1999). A two-fluid modelling of the hydrodynamics of the cocurrent gas-liquid trickle flow through a trickle-bed, *Chem. Eng. Sci.*, 54, 785-802.

Batchelor G.K. (1967). *An Introduction to Fluid Dynamics*, Cambridge University Press, N.Y.

Herskowitz M., & Smith J.M. (1983). Trickle bed reactors: A Review, *AIChE Journal*, 29, 1-18.

Melli T.R., de Santos J. M., Kolb W.B., & Scriven L.E. (1990). Cocurrent downflow in networks of passages. Microscale roots of macroscale flow regimes, *Ind. Chem. Res*, 29, 2367-2379.

Mewes D., Loser T., & Millies M. (1999). Modelling of two-phase flow in packings and monolits, *Chem. Eng. Sci*., 54 , 4729-4747.

Midoux N., Favier M., & Charpentier J-C. (1976). Flow pattern, pressure loss and liquid holdup data in gas-liquid downflow packed-beds with foaming and nonfoaming hydrocarbons, *J. of Chem. Eng. of Japan*, 9 (5), 350-356.

Nakoryakov V.E., Pokusaev B.G., & Shreiber I.R. (1993). *Wave Propagation in Gas-Liquid Media.* CRC Press, N.-Y.

Nigmatulin R.I. (1990). *Dynamics of Multiphase Flow*, vol. 1, 2 . Hemisphere, N.-Y.

Ng K.M. (1986). A Model for flow regimes transitions in cocurrent down-flow trickle-bed reactors, *AIChe Journal*, 32 (1), 115-122.

Rode S., Midoux N., Latifi M.A3., & Storck A. (1994). Multiple hydrodynamic states in trickle beds operating in high-interactions regimes: liquid saturation and flow regime transitions, *Chem. Eng. Sci*., 49, 2535-2540.

Rode S., Midoux N., & Storck A. (1995). Gas-liquid flow mechanisms in trickle beds operating in dispersed bubble and pulse flow, Trans. ICheme., 73, Part A, 275-279.

Sicardi S. , Gerhard H., & Hofmann H. (1979). Flow regime transition in trickle-bed reactors. *The Chemical Engineering Journal, 18,* 173-182.

Sicardi S., & Hofmann H. (1980) Influence of gas velocity and packing geometry on pulsing

inception in trickle-bed reactors. *The Chemical Engineering Journal*, 20, 251-253.